Deep Neural Network-based Current and Voltage Prediction Models for Digital Measuring Unit of Capacitive Resistivity Underground Imaging Transmitter Subsystem

Jonah Jahara Baun[1,3], **Adrian Genevie Janairo**[2,3], **Ronnie Concepcion II**[2,3], **Kate Francisco**[2,3], **Mike Louie Enriquez**[2,3], **R-Jay Relano**[2,3], **Edwin Sybingco**[1,3], **Argel Bandala**[1,3] and **Ryan Rhay Vicerra**[2,3]

[1]*Department of Electronics and Computer Engineering, De La Salle University, Manila, Philippines*
[2]*Department of Manufacturing Engineering and Management, De La Salle University, Manila, Philippines*
[3]*Center for Engineering and Sustainability Development Research, De La Salle University, Manila, Philippines*

Abstract: Real-time monitoring of output electrical parameters of the transmitted signals in a capacitive resistivity underground imaging system is necessary because these are significant in the calculation of underground resistivity, however, machine learning has not yet been applied in this application to improve the accuracy of measurement. This study aims to develop and select the best prediction models that can be implemented for a digital measuring unit suitable for capacitive resistivity underground imaging. Three deep neural network models namely Elman recurrent neural network (ERNN), long short-term memory (LSTM), and gated recurrent unit (GRU) were explored to build prediction models for the current and voltage of the transmitter circuit. The prediction models' performance was assessed using mean squared error (MSE), which is reduced to its absolute lowest value. The result shows that the best-trained models for current and voltage prediction are the ERNN models with configurations of 900-600-500 hidden neurons network with training MSE of 9.82×10^{-9} and the configured 1300-1000-900 hidden neurons with training MSE of 0.465, respectively. With the help of the prediction models, it would be possible to measure current and voltage output accurately, allowing simultaneous data acquisition while avoiding the need for a separate measuring device.

Keywords: Deep neural network, Recurrent neural network, Long short-term memory, Gated recurrent unit, Digital measuring circuit, Underground imaging

1. INTRODUCTION

Underground utility demand in the Philippines was projected to have an increasing trend as there is a constantly growing population rate from 1960 to 2021 with 26.27 million up to 111.05 million people, respectively [1]. Increasing population and industrial expansion both contribute to the establishment of various underground service utility lines such as pipes, water lines, electricity, and drainage [2]. With that, it introduces the exploration of utility and object detection through underground imaging technology to properly handle the web of utility lines. The study of underground imaging is necessary for the effective construction and operation of urban underground facilities [3]. This has been a well-known strategy since it has a non-destructive approach to detecting underground objects and structures, reducing the pre-construction process's adverse effects [2]. Specifically, a capacitive resistivity underground

imaging system is composed of a configured transmitter and receiver antennas that are capacitively coupled in the ground [4], [5] to measure the potential difference in resistivity readings [6]. The transmitter emits low-frequency electromagnetic waves into the ground and the multi-receiver systems will detect the reflected signals generated by a conductive anomaly [7]. Thus, this concept conveys that penetration, resolution capabilities, and frequency selection are incorporated into a well-configured antenna design.

Numerous designs of transmitter antennae appropriate for underground imaging have been developed over the years [8], [9]. In one investigation, a circular patch antenna that operates within 500 MHz and 2 GHz and is appropriate for GPR applications of detection of buried objects was used [10]. A high-power Gaussian monopulse ultrawideband transmitter for buried object detection was created using a different design that combined two pulse

generators based on Marx transistor, a Vivaldi antenna, and a balun [11]. Moreover, a transmitter unit which is a transverse electromagnetic flared (TEM) horn antenna with a pulse shaping circuit consisting of a crystal oscillator with an oscillation frequency of 10 MHz and an amplitude in the range of ±1 V has been developed for imaging of water pipelines [12]. Hence, in utilizing transmitter antenna design, one important factor is to monitor the current and voltage for verification of the parameters of output signals that are essential for the calculation of the subsurface resistivity, and this can be done through a measuring device such as the digital multimeter or an electrical measuring unit.

Digital multimeter (DMM) has various measuring capabilities such as Direct Current (DC) current/voltage, Alternating Current (AC) current/voltage, power, resistance, and electric energy [13]. Since it is a functional electronic device, it is crucial for the industry to further guarantee that the accurate and scientific process of electrical parameter measurements is observed. Thus, machine learning was used to boost the accuracy of digital measuring tools in recent years, leading to greater advancements, such as introducing a deep learning-based solution for reading recognition for digital multimeters using the You-Only-Look-Once (YOLO) detection approach in [14]. The display region along with important data was identified and extracted successfully which help in reducing maintenance procedure errors and maximizing the use of human resources. Another study proposed a digital multimeter reading recognition method that is based on machine learning for automation verification [15]. The verification method will be automated in the study in order to increase the effectiveness of power instrument detection. Then, in [16], this research investigates how deep learning neural network methods can be integrated to forecast voltage distribution in electrical power systems focusing on locating smart meters. Meanwhile, other electrical measures are not considered; this only predicts voltage magnitude. These studies showed the power of machine learning for electrical measuring equipment like digital multimeters. These algorithms can deliver accurate and real-time predictions by evaluating electrical measurements, which enables better monitoring and management of electrical systems.

According to multiple accounts, machine learning was used to develop prediction models for electrical parameters. In the study of [17], researchers compared neural network prediction models, support vector machine (SVM) for regression, and equation discovery for predicting the next voltage values without performing measurements. Another prediction modeling was employed through a convolutional neural network (CNN) to detect and categorize welding current to construct an ERT imaging trailer and detect defects [18]. While in [19], the paper suggests a prediction model of the input voltage signal received by an underground imaging system based on genetic programming (GP). Through this, the prediction model can replace laborious mathematical

calculations with a more accurate and effective approach. To forecast the charging level, voltage, current, speed, and mileage of lithium-ion batteries in electric vehicles, an artificial neural network (ANN) model is considered [20] while deep neural networks were already utilized for the prediction of battery life and voltage which addresses the challenges of lifetime and health prediction of batteries [21].

Nonetheless, the developed models cannot identify sequential data, therefore, time series forecasting models based on deep neural networks have been introduced to predict electrical parameters such as voltage and current based on historical data to optimize the prediction's accuracy. A deep recurrent neural network (DRNN) was effectively employed in estimating the consumption value of electricity in the medium to long-time frame [22]. Also, voltage instability of a power system has been successfully predicted using the recurrent neural network (RNN) with particle swarm optimization [23], and by employing an RNN thru long short-term memory (LSTM) [24] wherein it demonstrated promising results that are useful as a warning scheme for system operators. The remaining useful life (RUL) of electrical devices is predicted using a convolutional neural network integrated with long short-term memory (CNN-LSTM) network [25]. Non-linear voltages can be predicted by utilizing the LSTM network which is found to be accurate and effective [26]. Gated recurrent unit (GRU) has been introduced also which can be applied for estimating the charge state of lithium batteries in two different research [27], [28]. The first research algorithm employed the measured voltage and measured current as the input to predict the charge state while the other approach predicted the charge state by considering the measured temperature as the input. However, both showed higher prediction accuracy in predicting the SOC essential for battery management. In [29], the standard RNN, LSTM, and GRU models were compared to predict battery voltage. This study aims to identify the most effective model and to demonstrate the efficacy of RNN architectures in the specified task. Ultimately, it was determined that LSTM outperformed the other two frameworks by means of accuracy. Lastly, RNN, LSTM, and GRU were then explored to develop prediction models for estimating electrical load based on current measurements [30]. But, in this experiment conducted, the GRU model showed the highest potential regarding accuracy and the lowest error. Based on the aforementioned studies, the performance results of prediction models may vary depending on the nature of the dataset and the specific task at hand. To select the best model for a certain application including current and voltage prediction, more investigation and testing may be necessary. Also, there is no specific research that uses machine learning for the electrical system measurement of a capacitive resistivity underground imaging system.

In digital multimeters, it is important to consider the accuracy of electrical parameter readings to reduce and avoid deviation from their actual value. Additionally, there

is a need for real-time checking of the generated current and voltage by a single-pair antenna transmitter subsystem for underground imaging to verify the parameters of output signals in comparison to received signals of the receiver subsystem which is essential in calculating the underground's resistivity. Most significantly, machine learning methods have not yet been used to boost the accuracy of a digital multimeter designed for capacitive resistivity underground imaging equipment.

With that, the study focuses on the development of a prediction model that can be implemented for a digital measuring unit suitable for capacitive resistivity underground imaging applications. Particularly, three deep neural network models namely Elman recurrent neural network (ERNN), long short-term memory (LSTM), and gated recurrent unit (GRU) were explored to create time-series prediction models for current and voltage outputs of the transmitter circuit. To evaluate the performance of the developed prediction models and to select the best model with greater accuracy to predict the current and voltage, mean squared error (MSE) was used and reduced to its absolute minimum. Through the development of the current and voltage prediction model for the digital measuring unit, it will allow simultaneous data acquisition through a single connection from the transmitter of a single-pair antenna system for underground imaging. Also, these prediction models contributed to providing a more accurate output reading of current and voltage which avoids the utilization of a separate, bulky, and multiple connection measuring device. Also, predictive models may continuously build upon and adjust to sudden changes in the electrical system, producing predictions and measurements with greater accuracy.

2. Materials and Methods

This research involves five major steps in the development of prediction models of current-voltage digital meter for monitoring of transmitter subsystem for underground imaging (Fig. 1). It starts with the construction of the current-voltage measuring circuit connected to the transmitter circuit designed for underground imaging equipment, then simulation of the circuitry for the collection of measured current and voltage data based on measured DC input voltage (V_{dc}) and set operating frequency (f_o), followed by the development of the different deep neural network models specifically ERNN, LSTM, and GRU to be used in predicting the output current and voltage. After that, training, validation, and testing of deep neural network models were conducted, and lastly, the selection of the best neural network model with the lowest MSE and comparison of predicted results with the measured values.

A. Construction of Transmitter Measuring Circuit

A capacitive resistivity underground imaging system comprised of transmitter and receiver subsystems to obtain electrical measurements from the ground [8]. Prior to constructing a digital measuring circuit, a transmitter circuit is first designed, and it operates at frequencies ranging from

3.5 KHz to 18.5 KHz. The transmitter circuit can send out sine, triangular, or rectangular wave signals.
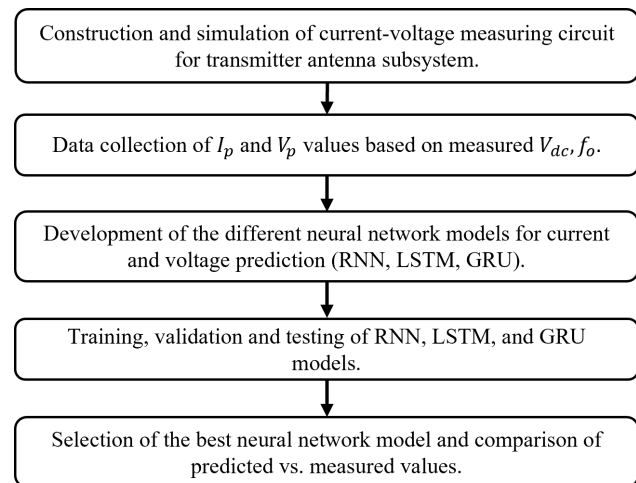
Figure 1. Step-by-step process of the prediction of current and voltage for digital measuring circuit to be used for monitoring the transmitted signals in capacitive resistivity underground imaging system

The range of output voltage from the transmitter is from 500 V_{pk} to 1500 V_{pk} with a minimum power of 2 W and a maximum power of 20 W. To achieve a 10 W output power, its corresponding output voltage must be 10 W. While at maximum power output, the maximum current is close to 15 mA.

The electrical parameters required for proper measurement and analysis of the resistivity of underground imaging using the capacitive resistivity technique are the transmitter's output current and voltage, and the receiver's in-phase voltage component reading [8]. These electrical measurements are essential for the computation of the ground equivalent resistance using Ohm's Law [31]. The digital measuring circuit, designed in this study, focused on acquiring only the measurements from the transmitter subsystem, therefore with the readings of the output current and voltage. Analog signal processing is used on the transmitter's output, and digital signal processing is done on the measurement circuit's output signal before it is sent to the Arduino. The key purpose of the constructed transmitter measuring circuit is to obtain the current and voltage signal levels from the output of the transmitter and convert it into signals that are within the input threshold of Arduino or any microcontroller, usually $0 - 3$ V. In the actual implementation of a capacitive resistivity underground imaging system, the current and voltage being transmitted to the ground cannot be determined without a measuring device being linked to it, thus, a digital measuring circuit is necessary as these transmitted amounts of current and voltage signals are valuable in data processing and analysis of underground's electrical properties.
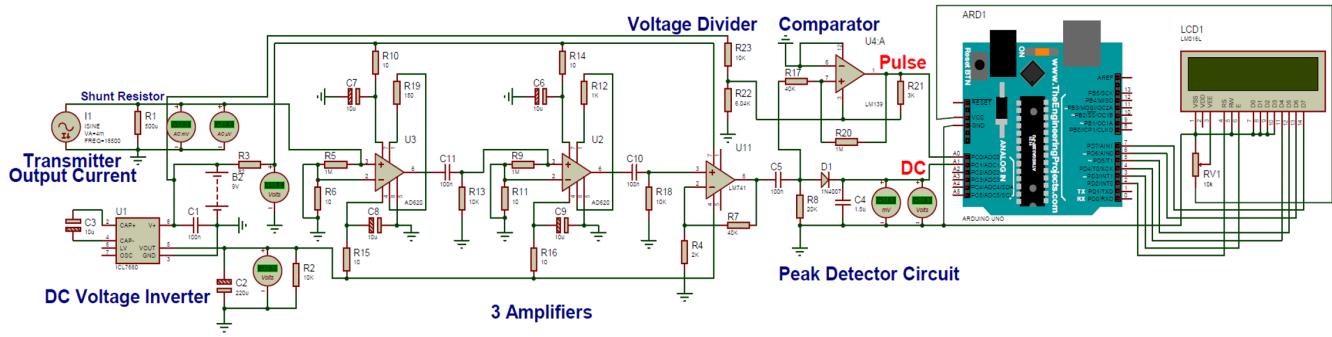
Figure 2. Transmitter digital measuring circuit designed using Proteus Simulation Software

The digital measuring circuit, which is designed and simulated using Proteus Software (Fig. 2), is composed of a 500 µΩ shunt resistor that is used for measuring and obtaining the transmitter output's current values, represented by a current source for an isolated simulation. Its corresponding AC voltage signal present at the shunt resistor is amplified with a gain of 322,641 using a 3-stage cascaded amplifier. The amplified AC voltage signal is then converted to a DC voltage signal using a peak detector circuit which served as an input in the A1 ADC pin of the Arduino. The DC voltage at the A1 10-bit ADC pin is measured and needed to be converted to its equivalent transmitter peak current, thus simulations were performed to compile relationships between the current and the measured DC voltage signal. Moreover, a parallel connection between the output of the 3-stage cascaded amplifier and a comparator circuit was created to generate pulse signals that have an output ranging from 0 to 2.5 V_{pk-pk}. This pulse signal then serves as an input to the Arduino using the A0 ADC pin which is useful so that the Arduino could read the measured signals. The LCD is then used for displaying the transmitter current and voltage.

B. Data Collection and Preparation

To consider the effect of the coupling and parasitic capacitances acting as filters that change the frequency response of the measuring circuit in capacitive resistivity underground imaging, different input signal frequencies were considered in the circuit simulation, and from that the transmitter output current can be represented not just as a function of the measured DC signal but also taking into account of operating frequency. The frequency is obtained from the pulses at the input signal of the A0 ADC pin. The first 139-row dataset was obtained from the circuit simulation by adjusting the values of transmitter output current through a current source as shown in Figure 2. Only 139 rows were gathered because the computer used for Proteus simulation experienced slow run time due to excessive Central Processing Unit (CPU) load and insufficient RAM. This resulting 139-row dataset contains the list of random values of signal operating frequencies ranging from 3.178 KHz to 18.5 KHz, corresponding measured DC input voltages ranging from 0.487 V_{dc} to 2.5 V_{dc}, and the equiv-

alent measured output current values of 4 mA to 15 mA. These three parameters of the first dataset were used for training the developed current prediction models whereas the input parameters used are the obtained measured DC input voltages and operating frequencies while the target output parameter is the measured output current from the measuring circuit.

With the established dataset for model training for current prediction, the next step is to acquire the relation of the transmitter output voltage to be defined by the predicted current to identify the specific parameters needed in training the voltage prediction models. Through the simulations performed with the transmitter circuit, it was observed that the relationship between the output voltage and current was not perfectly linear, therefore there is a need to generate another dataset for peak voltage prediction to lessen the error compared to an MSE of 62 from simply multiplying the predicted current with the average computed circuit load of 102.54 Ω. From the simulation, the second dataset is composed of 419 rows of relationships of the transmitter output currents and voltages ranging from 4 mA to 15 mA and 411 V_{pk} to 1485 V_{pk}, respectively. These parameters were used to train the voltage prediction models wherein the measured current from the transmitter circuit's output is used as the input parameter, and the measured voltage is the target output.

C. Recurrent Neural Network Modeling

Advanced deep learning prediction and classification techniques called recurrent neural networks (RNNs) are especially effective at dealing with time-series information along with other data sets that are sequential [32] that perform well and most sophisticated method for machine learning, and natural language processing [33]. Typically, an RNN's hidden state h_t dynamics given an input sequence $x = x_1, x_2, ..., x_t$ may be expressed as:

$$h_t = \begin{cases} 0, & if(t = 0) \\ \emptyset(h_{t-1}, x_t), & otherwise \end{cases} \quad (1)$$

where $\emptyset$ is a non-linear function while the updated recurrent

hidden state is stated as follows:

$$h_t = \sigma(Wx_t + Uh_{t-1}) \tag{2}$$

where σ is a hyperbolic tangent function, W is the input neuron weight, and U is the recurrent neuron weight. Thus, the output Z at time t is calculated as:

$$Z_t = (Wh_y + h_t) \tag{3}$$

where Wh_y is the corresponding weight at the output layer.

In this study, the prediction of the current level has been performed specifically using the Elman recurrent neural network (ERNN) architecture presented in Figure 3 whereas there are two inputs (DC input voltage and operating frequency), three hidden layers, and one expected output for predicted current.
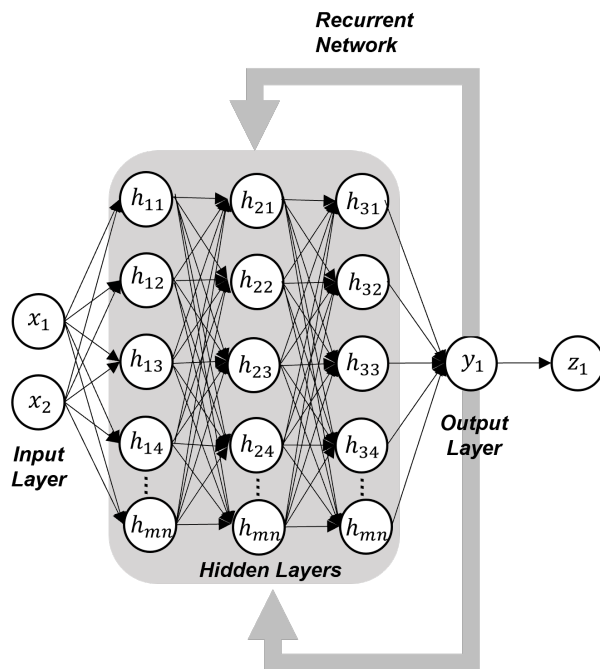
Figure 3. The designed Elman recurrent neural network architecture for current signal prediction

D. Long Short-Term Memory

The long short-term memory (LSTM) model was deep neural network created to address the inadequacies of RNNs, for the purpose of capturing long-term information and improving performance on long sequence data [34], To overcome the problems of disappearing gradients and gradient expansion, LSTM introduces input gates and forget gates [35].

The LSTM layers are comprised mainly of four gates that manipulate the cell-state data. The first is referred to as the "forget gate," which recognizes and omits data that is optional and not necessary. The sigmoid function also specifies which of the previous output can be removed. The input gate comes next, where the sigmoid function determines whether or not the data will be written. The next layer is the candidate gate with the tanh functions that weigh the importance of the data and control what to write in the cell state. The output gate then determines what information should be delivered as the output concealed state h_t after filtering the new values generated by the tanh layer from the cell state c_t with the sigmoid function [36]. The cell state is in charge of adding or eliminating previous data based on its relevance and importance in making the forecast [34].

$$i_t = \sigma(x_t U^i + h_{t-1} W^i) \tag{4}$$

$$f_t = \sigma(x_t U^f + h_{t-1} W^f) \tag{5}$$

$$o_t = \sigma(x_t U^o + h_{t-1} W^o) \tag{6}$$

In (4) to (6), i_t, f_t, o_t represent the input gate, forget gate, and output gate where σ is the sigmoid function, x_t is the input given, U^i, U^f, and U^o, represent the weight of the input in the input, forget, and output gates respectively, h_{t-1}, holds the data from the preceding terms, while W^i, W^f, and W^o are the weights of the data from the preceding terms in the input, forget, and output gates. Then, the cell state c_t is given to tanh function and multiplied to o_t to get the updated hidden state h_t.

E. Gated Recurrent Unit

The gated recurrent unit (GRU) is a specific kind of optimized deep LSTM-based recurrent neural network that keeps the LSTM immunity to the vanishing potential problem. Updating the internal states requires less work since the underlying structure is simpler and easier to train. The reset port decides whether the current state should be coupled with the prior information, while the update port governs how much of the state data from the last instant is maintained in the present condition. GRU requires less memory and is quicker than LSTM. However, when working with datasets that comprise longer sequences, LSTM is accurate to a greater extent [35]. GRU's input and output structures are identical to those found in a standard RNN, while its internal structure is comparable to an LSTM [35]. A typical GRU is composed of reset gate r and update gate textitz which can be calculated as:

$$r_t = \sigma(x_t W_r + h_{t-1} U_r) \tag{7}$$

$$z_t = \sigma(x_t W_z + h_{t-1} U_z) \tag{8}$$

where σ is the sigmoid function, x_t is the given input, W_r and W_z are the weights in the input of the reset and update gate, respectively, h_{t-1} holds the data of the preceding units while U_r and U_z represent the weights of the preceding units in the reset and update gate, accordingly. Finally, the hidden state h_t is calculated using the hidden state of time t-1 and input time series value x_t.

Additionally, the LSTM and GRU architecture for current prediction used in this study is presented in Figure 4 It represents two inputs (DC input voltage and operating frequency), three hidden layers, a fully connected layer, and one expected output for predicted current.
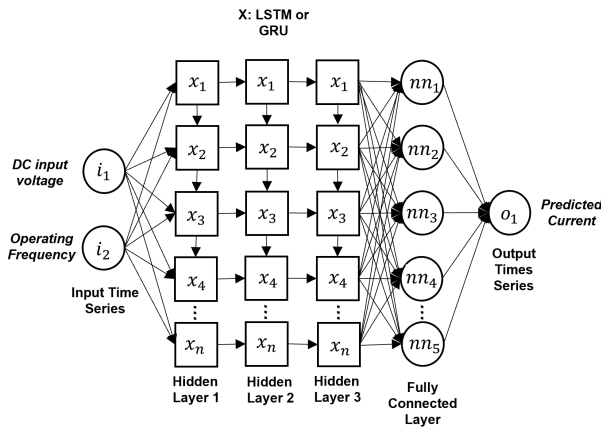
Figure 4. The designed LSTM and GRU network architecture for current signal prediction

F. Peak Voltage and Peak Current Prediction using ERNN, LSTM, and GRU

The three deep neural networks, specifically, ERNN, LSTM, and GRU, were coded and performed using MAT-LAB Software. The ERNN was modeled using the hyperparameters presented in Table I while LSTM and GRU are shown in Table II. Each of the three deep neural network models is composed of three hidden layers wherein in hidden layer 1, the simulated number of neurons was set to 500, 700, 900, 1100, and 1300, in hidden layer 2 was 200, 400, 600, 800, 1000, and in hidden layer 3 was 100, 300, 500, 700, 900. The three models each received 500, 1000, 1500, 2000, and 2500 training epochs.

The logarithmic transfer function 'logsig' has been applied as the function of activation for each hidden layer in the optimum network architecture in ERNN, linear transfer function 'purelin' has been applied to the output layer, while 'trainrp' is used as the network training function by which in accordance with the resilient backpropagation method, it adjusts the values of the weights and biases.

To update the parameters of the network in a custom training loop in LSTM and GRU model for current prediction, the stochastic gradient descent with momentum

(SGDM) algorithm was applied. On the other hand, for voltage prediction, the adaptive moment estimation optimizer (ADAM) was employed. Lastly, LSTM and GRU models also employed an initial rate of learning of 0.01 and 128 as the minibatch size.

TABLE I. Hyperparameters for Current and Voltage Predictions using ERNN

Hyperparameter	Value
1st Layer Number of Neurons	500, 700, 900, 1100, 1300
2nd Layer Number of Neurons	200, 400, 600, 800, 1000
3rd Layer Number of Neurons	100, 300, 500, 700, 900
Number of Training Epochs	500, 1000, 1500, 2000, 2500
1st Layer Activation Function	Logsig
2nd Layer Activation Function	Logsig
3rd Layer Activation Function	Logsig
Output Layer Activation Function	Purelin
Training Function	Trainrp

TABLE II. Hyperparameters for Current and Voltage Predictions using LSTM and GRU

Hyperparameter	Value
1st Layer Number of Neurons	500, 700, 900, 1100, 1300
2nd Layer Number of Neurons	200, 400, 600, 800, 1000
3rd Layer Number of Neurons	100, 300, 500, 700, 900
Number of Training Epochs	500, 1000, 1500, 2000, 2500
Optimizer/Training Function	SGDM/ADAM
Initial Learning Rate	0.01
Minibatch Size	128

G. Prediction Model Evaluation Metric

Since the study is a regression task, thus, one specific evaluation metric design used to assess the prediction models' performance is the Mean Squared Error (MSE). This indicator provides a measurement of how well the model works in terms of prediction accuracy by measuring the error or a disparity between predicted and actual values.

The MSE between the actual and predicted values for each output node in relation to network training was used to determine the performance of the three deep neural networks. It is expressed mathematically as:

$$MSE = \frac{1}{n} \sum_{i=1}^{n} Y_i - \hat{Y}_i \qquad (9)$$

where n is the data points number, Y_i is the actual values, and $\hat{Y}_i$ is the predicted values.

3. RESULTS AND DISCUSSION

A. Relationship of the Electrical Antenna Parameters

To ascertain the degree of relationship between the transmitter antenna operating frequency, DC input voltage, and the resulting antenna current, a Pearson correlation analysis with a 95% confidence level was carried out. In the Minitab platform, two parallel coordinate charts were created to

clarify the non-linear relationships of the relevant antenna electrical characteristics (Fig. 5). The peak current and peak voltage ratings have an extremely positive correlation (R^2 = 1) and the antenna transmitter DC input voltage (V_{DC}) has a very strong positive correlation with the output current (R^2 = 0.956) which suggests that V_{DC} is a highly significant input parameter that could potentially alter the receiver voltage readings, especially with composite air and biomaterials as dielectric. On the other hand, the operating frequency of the transmitter has weak negative (R^2 = -0.134) and weak positive (R^2 = 0.129) impacts on V_{DC} and output current which confirmed that it is only responsible for the degree of resolution in the receiver side, however, it should be properly calibrated to assure capacitive resistivity operation.
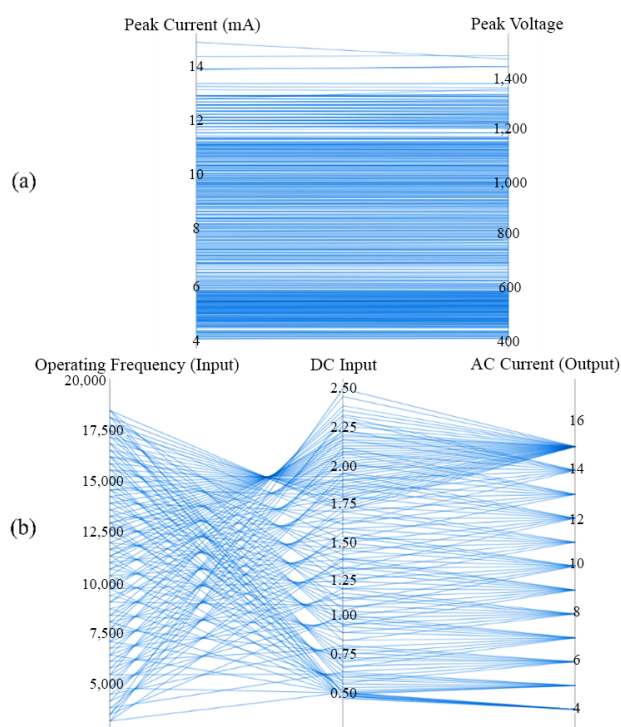
Figure 5. Parallel coordinate plots (a) between peak current and voltage ratings, and (b) among operating frequency, DC input voltage, and output current of the transmitter antenna

B. Simulation Comparison of Current Prediction Models

The simulated current prediction models in MATLAB Software using ERNN, LSTM, and GRU are shown in Table III. In this paper, 25 configurations of ERNN current prediction models have been trained. To train the different model combinations, The 139 patterns input-output dataset was separated into three distinct sets at random: a training data set, which makes up 56% of the data, a validation data set, which makes up 24% of the data, and a test data set, which makes up 20% of the data. The input parameter used for current prediction is the obtained measured DC input voltages of the transmitter circuit and set operating

frequency ranging from 3.5 KHz to 18.5 KHz and the target output parameter is the measured current from the measuring circuit. The training target error performance was set to 1×10^{-8}. It can be observed that the trained model with hidden neuron combination of 500-200-100 and some of the trained configurations have a rapid elapsed time of less than 100 seconds due to the vanishing or exploding gradient descent encountered during training by which it is evident that one of the drawbacks of RNN is that when the network is unfolded for an excessive number of time steps or when it is processing the lengthy sequential data used in this study, the gradient of some of the weights tends to become overly small or big [37]. Due to the gradient's shifting weight, if the weight has been set low enough, the gradient will vanish and the hidden layer next to the input layer will discontinue learning. On the other side, a weight that is excessively large will result in a rapid increase in the gradient. RNN lacks long-term memory, so it is sensitive to time steps and will be impacted by short-term memory [35]. Moreover, six out of the 25 trained ERNN models have almost met the performance criterion of 1×10^{-8}. For the current prediction ERNN model, the combination of 900-600-500 hidden neuron network models with training epochs of 2,500 has the lowest MSE during training.

Another 25 configured networks of LSTM models have been trained also for the current prediction. The simulated current prediction models using LSTM are presented (Table III). For the input-output dataset, the 139 rows of sequential data for current prediction are divided into three: 80% for the training data, 10% as validation data, and the remaining 10% as testing data. The 'SGDM' optimizer performed well as the training function for the current prediction dataset because it helps to accelerate gradient vectors in the correct directions, which causes short sequential data to converge more rapidly. From the perspective of the training time, the average running time of the LSTM model for the current prediction is 444.48 seconds. Although there are networks with less than 100 seconds of elapsed time, the LSTM models have solved the issue of vanishing or exploding gradient descent [35]. All the configured networks completed the learning process. Thus, the combination of 900-600-500 hidden neurons with 2500 training epochs achieved the lowest training MSE for the LSTM network.

The GRU models for current prediction are comprised also of 25 different networks presented in Table III. Similar to LSTM, the input-output dataset included 139 rows of sequential data that were split into 80% training data, 10% data for validation, and the other 10% of data for testing. Since GRU is also proven to address concerns with exploding or vanishing gradient descent. All network models were learned with an average running time of 763.56 seconds. This shows that the GRU models have a slower average training time than the LSTM because the simulated networks are comprised of a complex and larger number of parameters. Hence, the 500-200-100 hidden neuron network

TABLE III. Simulated Current Prediction Models using ERNN, LSTM, and GRU

Layer 1	Layer 2	Layer 3	Epochs	ERNN		LSTM		GRU	
				Train MSE	Run Time (s)	Train MSE	Run Time (s)	Train MSE	Run Time (s)
500	200	100	500	4.41×10^{-4}	23	1.910	55	0.861	73
500	200	100	1000	1.39×10^{-7}	51	0.897	107	0.877	135
500	200	100	1500	1.28×10^{-5}	74	0.933	162	0.795	203
500	200	100	2000	4.21×10^{-5}	97	0.985	156	0.990	278
500	200	100	2500	9.90×10^{-8}	49	0.847	222	0.938	338
700	400	300	500	2.83×10^{-5}	57	1.030	107	0.892	187
700	400	300	1000	1.19×10^{-5}	114	1.020	227	0.942	312
700	400	300	1500	3.32×10^{-6}	166	0.906	224	0.796	429
700	400	300	2000	9.98×10^{-8}	194	1.030	334	0.870	597
700	400	300	2500	3.13×10^{-6}	274	0.988	384	0.798	644
900	600	500	500	2.52×10^{-5}	107	0.981	136	0.932	228
900	600	500	1000	2.43×10^{-6}	219	0.875	181	0.898	471
900	600	500	1500	6.08×10^{-5}	312	1.080	415	0.807	631
900	600	500	2000	9.98×10^{-8}	326	0.949	537	0.933	782
900	600	500	2500	9.82×10^{-9}	354	0.845	592	0.978	1130
1100	800	700	500	6.63×10^{-2}	178	1.060	179	0.861	362
1100	800	700	1000	1.18×10^{-4}	347	1.210	200	0.949	694
1100	800	700	1500	6.04×10^{-6}	532	0.959	513	1.030	1066
1100	800	700	2000	1.80×10^{-4}	725	1.030	717	0.881	1414
1100	800	700	2500	6.13×10^{-7}	873	0.966	905	0.834	1825
1300	1000	900	500	9.03×10^{-5}	259	0.883	270	0.989	496
1300	1000	900	1000	5.31×10^{-5}	561	1.020	598	0.849	1026
1300	1000	900	1500	9.95×10^{-8}	581	0.895	870	0.868	1512
1300	1000	900	2000	6.38×10^{-4}	1047	0.860	1191	0.961	1850
1300	1000	900	2500	9.99×10^{-8}	998	0.917	1830	7.710	2424

with 1500 training epochs attained the lowest training MSE since GRU is more accurate and faster with fewer training parameters and a smaller dataset. Additionally, considering the model principle, GRU can disremember and pick memories with just one gate, since there is less number of neurons in a 500-200-100 hidden neuron network with shorter training epochs, it accomplishes the task with greater efficiency and precision than the other configurations [35].

C. Simulation Comparison of Voltage Prediction Models

The simulated voltage prediction models using ERNN, LSTM, and GRU are presented in Table IV. There are also 25 configured networks for each of the ERNN, LSTM, and GRU. In order to forecast the voltage using ERNN, 419 series of measured current from the transmitter circuit's output are used as the input data, and the matching 419 series of measured voltage is utilized as the target output dataset. These 419 datasets were divided into 56% for training, 24% for validation, and 20% for testing. Similar to the current ERNN prediction models, the training target error performance was set to 1×10^{-8} and all the ERNN combinations of 500-200-100 hidden neurons and other trained configurations also experienced a rapid training elapsed time because of the vanishing gradient descent wherein to calculate the gradients with respect to the features in the hidden layers of the preceding time step should need an extensive amount of computation [37]. However, the ERNN combination of 1300-1000-900 hidden neurons with 2000 training epochs met the lowest training MSE for this network.

Furthermore, the simulated voltage prediction models using LSTM are given in Table IV. In the following networks, the same as ERNN, the 419 input-output datasets were also applied for the training, validation, and testing. These 419 rows are divided into 80% training data, 10% validation data, and 10% testing data. The average running time of the training period for voltage prediction using LSTM is 775.6 seconds. Also, the chosen 'ADAM' optimizer for voltage prediction worked well as the training function since it is appropriate for the optimization of larger datasets [38]. The problem with vanishing or exploding gradient descent of RNN voltage prediction models was also addressed by the LSTM voltage prediction models. Therefore, the 900-600-500 hidden neuron combination of 2500 training epochs attained the lowest possible training MSE.

Lastly, the simulated GRU voltage prediction models are shown in Table IV. The 419 input-output datasets were also applied for the training, validation, and testing. These 419 rows are divided into 80% training data, 10% validation data, and 10% testing data. The average running time of the training period for voltage prediction using GRU is 1189.09 seconds which is slower than the LSTM, but the best GRU network is the same results as the LSTM current prediction model which is the 500-200-100 hidden neuron combination of 1500 training epochs.

TABLE IV. Simulated Voltage Prediction Models using ERNN, LSTM, and GRU

Layer 1	Layer 2	Layer 3	Epochs	ERNN		LSTM		GRU	
				Train MSE	Run Time (s)	Train MSE	Run Time (s)	Train MSE	Run Time (s)
500	200	100	500	8.23×10^{-4}	4	5.69×10^4	91	1.02×10^5	134
500	200	100	1000	7.84×10^{-7}	5	335	197	8.34×10^4	165
500	200	100	1500	7.59×10^{-5}	4	163	289	8.12×10^4	206
500	200	100	2000	8.37×10^{-5}	4	112	290	8.06×10^4	327
500	200	100	2500	7.55×10^{-8}	4	112	376	2.12×10^3	407
700	400	300	500	3.230	85	182	139	7.93×10^4	198
700	400	300	1000	2.210	168	283	317	7.98×10^4	372
700	400	300	1500	1.410	256	98	473	7.99×10^4	557
700	400	300	2000	1.460	332	21	641	8.89×10^4	670
700	400	300	2500	1.940	471	31	744	8.37×10^4	944
900	600	500	500	2.890	177	244	234	8.02×10^4	320
900	600	500	1000	5.770	330	51	467	8.28×10^4	655
900	600	500	1500	1.550	569	27	623	8.74×10^4	984
900	600	500	2000	1.730	12	27	1017	8.32×10^4	1252
900	600	500	2500	1.190	898	16	1175	8.03×10^4	1739
1100	800	700	500	1.720	272	89	391	8.47×10^4	535
1100	800	700	1000	6.900	600	53	698	7.97×10^4	1168
1100	800	700	1500	0.523	889	54	1050	8.24×10^4	1788
1100	800	700	2000	0.834	1243	23	1278	8.24×10^4	2219
1100	800	700	2500	1.160	47	24	1802	8.25×10^4	2700
1300	1000	900	500	1.210	380	153	512	8.19×10^4	830
1300	1000	900	1000	0.717	808	36	971	8.34×10^4	1683
1300	1000	900	1500	0.909	63	134	1458	1.10×10^5	2319
1300	1000	900	2000	0.465	552	33	1852	8.14×10^4	3346
1300	1000	900	2500	0.915	1053	31	2305	8.09×10^4	4209

D. Evaluation of RNN, LSTM, and GRU Model Performance

The best deep neural network models for each of the simulated ERNN, LSTM, and GRU for current and voltage prediction were consolidated in Table V and Table VI, respectively. After training the different networks, the selected best models were validated and tested. For the prediction of current, the results (Table V) reveal that the ERNN of 900-600-500 hidden neuron combination of 2500 training epochs outperformed the LSTM and GRU models with the lowest training MSE of 9.82×10^{-9} and a validation MSE of 1.26×10^{-8} which is lower than the test MSE of 0.587. Therefore, this configuration is selected as the best-trained model in predicting the current for the current measuring circuit of the transmitter antenna applied in underground imaging. This also shows that the ERNN provides better accuracy than the two other models due to the training hyperparameters and length of data samples.

Same with predicting the voltage, the best-simulated models for ERNN, LSTM, and GRU are shown in Table 6. From that, it has been proven that the ERNN has also bested the LSTM and GRU results. The ERNN model of 1300-1000-900 hidden neuron combination with 2000 training epochs has the lowest training MSE of 0.465, validation MSE of 0.659, and test MSE of 0.751, thus, it is selected as the best-trained model for the application of this study in predicting the voltage for measuring circuit of transmitter antenna used in underground imaging.

To visualize the actual current from the transmitter antenna and the predicted current generated by the three best-trained models, the scatter plot with the regression line of the three models (ERNN, LSTM, GRU) is presented in Figure 6 with the predicted and actual current values obtained during model training. The selected best-trained ERNN model with 900-600-500 hidden neuron network of 2500 training epochs presented the best fit for the data (Fig. 6a) since the points are close to the regression line implying that the predicted values are close to the actual values. Conversely, the scatter plot of the predicted and actual values generated by the best-trained LSTM and GRU models (Fig. 6a and Fig. 6c) are not visually appealing and did not present a good fit since there are points that are far from the regression line indicating slightly large discrepancies between the predicted and actual current values.

In Figure 7, the comparison of actual output peak voltage from the transmitter and predicted voltages produced by the three models (ERNN, LSTM, GRU) is visualized through a scatter plot graph. The chosen optimum trained ERNN model with 1300-1000-900 hidden neuron network of 2000 training epochs provided the best fit for the actual voltage values against the predicted voltage values (Fig. 7a). Its plot displays the points that are close to the regression line. However, it is evident that the two other voltage prediction models did not provide a good fitting for the actual and predicted voltage. Figure 7b and Figure 7c, respectively, of the scatter plots for the LSTM and

TABLE V. Best Models for Simulated ERNN, LSTM, and GRU Networks for the Current Prediction

Model	Layer 1	Layer 2	Layer 3	Epoch	Train MSE	Validation MSE	Test MSE
ERNN	900	600	500	2500	9.82×10^{-9}	1.26×10^{-8}	0.587
LSTM	900	600	500	2500	0.845	1.06	1.51
GRU	500	200	100	1500	0.795	1.42	1.42

TABLE VI. Best Models for Simulated ERNN, LSTM, and GRU Networks for the Voltage Prediction

Model	Layer 1	Layer 2	Layer 3	Epoch	Train MSE	Validation MSE	Test MSE
ERNN	1300	1000	900	2000	0.465	0.659	0.751
LSTM	900	600	500	2500	1.60	1.36	1.49
GRU	500	200	100	1500	2120	1690	2860
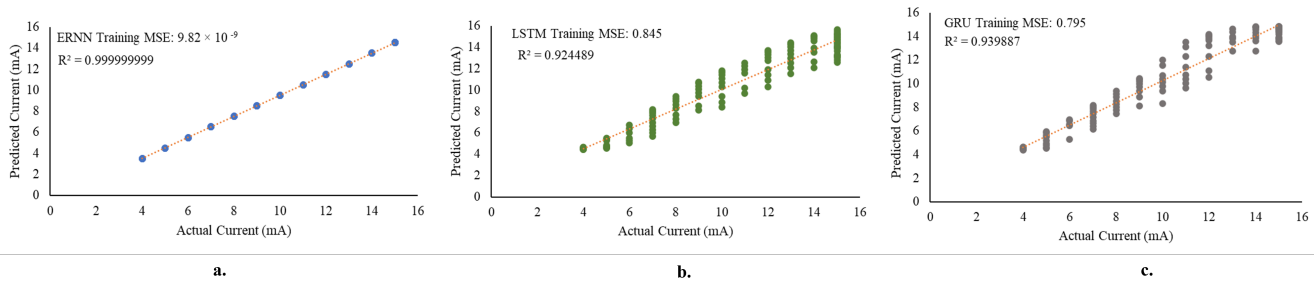
Figure 6. The scatter plot of the actual current from the transmitter antenna circuit against the predicted current obtained from: a). 900-600-500 ERNN network, b.) 900-600-500 LSTM network, and c.) 500-200-100 GRU network
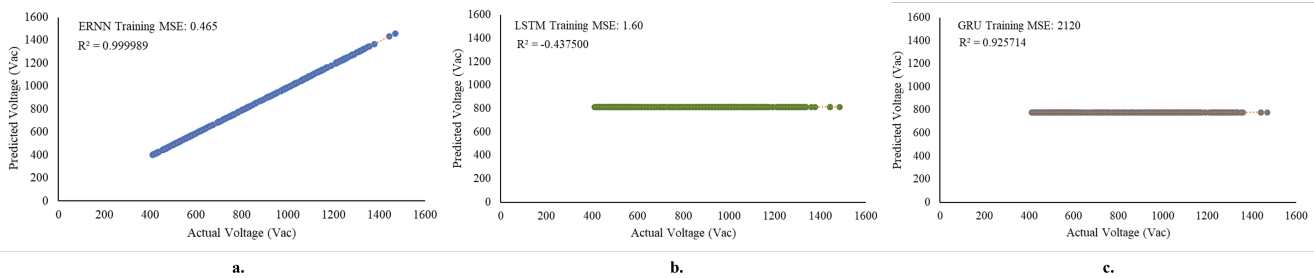
Figure 7. The scatter plot of the actual voltage from the transmitter antenna circuit against the predicted voltage obtained from: a). 1300-1000-900 ERNN network, b.) 900-600-500 LSTM network, and c.) 500-200-100 GRU network

GRU models, illustrate that the predicted values are almost constant, indicating that the regression models are unable to capture the hidden trends in the data, leading to poor fit of the models and failure to generalize new data. Although the LSTM training MSE is small, the value of R^2 is negative which is possible in some case, and it indicates that the model did not successfully learn the data's pattern providing a constant function that always predict the mean value of the voltage dataset. Therefore, the best-trained LSTM as well as GRU model is not appropriate to be selected as the voltage prediction model in this work.

The results show that the selected ERNN models have the minimum MSE and better accuracy closer to the actual value of current and voltage signals which is essential compared to manual computations of output parameters through Ohm's Law and it is proven that RNN works effectively as presented in [16], [18] by its ability to estimate reference voltage for monitoring purposes without actually performing any measurements and in predicting electrical parameters. Compared with LSTM and GRU, the ERNN model has the ultimate advantages of fast training speed and lower predictive error in this application. This study shows that, depending on the specific prediction task, ERNN remains capable of outperforming the other two models as opposed to [29], [30], where LSTM and GRU delivered the maximum prediction accuracy. The parameters that are selected and the overall amount of data may have an impact on the outcomes since RNN often works better on large datasets and with complex training hyperparameters, as

prior research publications have demonstrated, and because its structure comprises feedback connections/weights that induce its memory attribute [39]. This also implies that the selected model can be implemented on the Arduino-based current measuring circuit allowing simultaneous data acquisition through a single connection, however, the computational cost is significantly affected by how the ERNN model is implemented given that it is a huge network that needs higher computational processing. With that, the MATLAB Software was also not able to convert the ERNN code into its corresponding MEX function and Arduino language for execution purposes. For future studies, the researchers would like to consider actual implementation of the selected models by changing the microcontroller with a better hardware interface, high resolution, and more powerful processing capabilities.

4. Conclusion and Future Works

In this study, a prediction model for the current and voltage of a designed digital measuring unit of a capacitive resistivity underground imaging system is developed. Specifically, different deep neural network models were investigated to predict the output current and peak voltage from the transmitter circuit. These three deep neural network models are Elman recurrent neural network (ERNN), long short-term memory (LSTM), and gated recurrent unit (GRU) which are designed and simulated in MATLAB software. For the current prediction, the dataset comprised of 139 rows. The input data used are the measured DC input voltages obtained from the simulated digital measuring circuit and the operating frequency of the transmitter circuit ranging from 3.5 KHz to 18.5 KHz while the output datasets are the measured output current of the transmitter circuit. On the other hand, in predicting the output peak voltage of the transmitter circuit, the input and output dataset is composed of 419 rows of transmitter peak currents and corresponding voltages ranging from 4 mA to 15 mA and 411 V_{pk} to 1485 V_{pk}, respectively. There are 25 configurations simulated for each of the ERNN, LSTM, and GRU networks with different combinations of hidden neurons on each of their three hidden layers and various training epochs. Based on the lowest MSE, the performance of the prediction models was evaluated. The results show that the ERNN models both for current and voltage prediction provide the optimum accuracy with the lowest MSE. The ERNN model with a 900-600-500 hidden neuron network trained at 2500 epochs outperformed the LSTM and GRU models with the lowest training MSE of 9.82×10^{-9} and a validation MSE of 1.26×10^{-8} which is lower than the test MSE of 0.587 in the prediction of output current. Additionally, the ERNN has also bested the LSTM and GRU results in predicting the output peak voltage of the transmitter circuit. The configured 1300-1000-900 hidden neuron network ERNN model trained at 2000 training epochs has the lowest training MSE of 0.465, validation MSE of 0.659, and test MSE of 0.751. The chosen best-trained models are deemed to be acceptable and offered a more accurate output reading of current and

voltage, avoiding the use of a separate, large, and multiple connection measuring device. Additionally, the ERNN algorithm of the best-trained models can be integrated into the actual development of the hardware and software of the transmitter digital measuring unit of a capacitive underground imaging system, thus, enabling simultaneous data acquisition through a single connection only from the transmitter subsystem. However, the developed models have not been tested in either simulation or actual set-up because the Arduino microcontroller used in the circuit simulation has limited processing power and memory to perform the required high computational processing of ERNN model while MATLAB was also not able to convert the ERNN algorithm into its corresponding MEX function and Arduino language for execution purposes. Machine learning on an Arduino board might need some more work and optimization. Therefore, the next stage for this study is the actual implementation of the selected best models by utilizing more advanced and high-powered microcontrollers. It is also advisable to retrain the model with a new set of data or adjust the parameters to improve the accuracy and reliability particularly for the actual implementation.

References

[1] W. D. Info, "Population growth in the philippines." [Online]. Available: https://www.worlddata.info/asia/philippines/populationgrowth.php

[2] H. M. Jeong and D. M. Abraham, "A decision tool for the selection of imaging technologies to detect underground infrastructure," *Tunnelling and Underground Space Technology*, vol. 19, pp. 175–191, 2004.

[3] W. W. Lai, "Underground utilities imaging and diagnosis," *Urban Informatics*, pp. 415–438, 2021.

[4] A. G. Janairo, J. J. Baun, R. Concepcion, R. Relano, K. Francisco, M. L. Enriquez, A. A. Bandala, R. R. P. Vicerra, M. I. Alipio, and E. P. Dadios, "Optimization of subsurface imaging antenna capacitance through geometry modeling using archimedes, lichtenberg and henry gas solubility metaheuristics," *2022 IEEE International IOT, Electronics and Mechatronics Conference (IEMTRONICS)*, 2022.

[5] K. Francisco, R. Relano, M. L. Enriquez, R. Concepcion, J. J. Baun, A. G. Janairo, R. R. P. Vicerra, A. A. Bandala, E. P. Dadios, and J. R. Dungca, "Systematic analysis and proposed ai-based technique for attenuating inductive and capacitive parasitics in low and very low frequency antennas," *2022 IEEE International IOT, Electronics and Mechatronics Conference (IEMTRONICS)*, 2022.

[6] K. Francisco, R. Concepcion, R. Relano, M. L. Enriquez, J. J. Baun, A. P. Mayol, J. L. Espanola, R. R. P. Vicerra, A. A. Bandala, E. P. Dadios, A. T. Ubando, and H. Co, "Analytical hierarchical process-based material selection for trailer body frame of an underground imaging system," *2021 IEEE 13th International Conference on Hu-*

manoid, Nanotechnology, Information Technology, Communication and Control, Environ, 2021.

[7] L. L. Monte, F. Soldovieri, D. Erricolo, and M. C. Wicks, "Imaging below irregular terrain using rf tomography," *IEEE Transactions on Geoscience and Remote Sensing*, vol. 50, pp. 3364–3373, 2012.

[8] O. Kuras, D. Beamish, P. Meldrum, and R. Ogilvy, "Fundamentals of the capacitive resistivity technique," *Geophysics*, vol. 71, pp. G135–G152, 2006.

[9] R. D. Ogilvy, P. I. Meldrum, O. Kuras, and D. Beamish, "Systems and methods for resistivity measurement," 2009.

[10] M. N. A. Karim, M. F. A. Malek, M. F. Jamlos, L. Y. Seng, and N. Saudin, "Design of ground penetrating radar antenna for buried object detection," in *2013 IEEE International RF and Microwave Conference (RFM)*, 2013, pp. 253–257.

[11] M. Alesheikh, R. Feghhi, F. M. Sabzevari, A. Karimov, M. Hossain, and K. Rambabu, "Design of a high-power gaussian pulse transmitter for sensing and imaging of buried objects," *IEEE Sensors Journal*, vol. 22, pp. 279–287, 2022.

[12] M. Bimpas, A. Amditis, and N. K. Uzunoglu, "Design and implementation of an integrated high resolution imaging ground penetrating radar for water pipeline rehabilitation," *Water Resources Management*, vol. 25, pp. 1239–1250, 2010.

[13] K. Tingting, L. Yan, Z. Lei, and H. Yan, "Development of multichannel automatic digital multimeter calibration device," in *2019 14th IEEE International Conference on Electronic Measurement Instruments (ICEMI)*, 2019, pp. 108–113.

[14] W. Zhou, J. Peng, and Y. Han, "Deep learning-based intelligent reading recognition method of the digital multimeter," in *2021 IEEE International Conference on Systems, Man, and Cybernetics (SMC)*, 2021, pp. 3272–3277.

[15] W. Mo, L. Pei, Q. Huang, and L. Weijie, "Digital multimeter reading recognition for automation verification," *Proceedings of the 2nd International Conference on Artificial Intelligence and Advanced Manufacture*, 2020.

[16] M. Mokhtar, V. Robu, D. Flynn, C. Higgins, J. Whyte, C. Loughran, and F. Fulton, "Prediction of voltage distribution using deep learning and identified key smart meter locations," *Energy and AI*, vol. 6, p. 100103, 2021.

[17] I. Nancovska, D. Fefer, and A. Jeglic, "Predictive models for voltage reference elements monitoring," in *IMTC 2001. Proceedings of the 18th IEEE Instrumentation and Measurement Technology Conference. Rediscovering Measurement in the Age of Informatics (Cat. No.01CH 37188)*, vol. 3, 2001, pp. 1596–1601 vol.3.

[18] M. L. Enriquez, R. Concepcion, R.-J. Relano, K. Francisco, A. P. Mayol, J. Española, R. R. Vicerra, A. Bandala, H. Co, and E. Dadios, "Prediction of weld current using deep transfer image networks based on weld signatures for quality control," in *2021 IEEE 13th International Conference on Humanoid, Nanotechnology, Information Technology, Communication and Control, Environment, and Management (HNICEM)*, 2021, pp. 1–6.

[19] J. J. Baun, A. G. Janairo, R. Concepcion, K. Francisco, M. L. Enriquez, R.-J. Relano, J. A. de Leon, A. Bandala, R. R. Vicerra, and J. Dungca, "Hybrid stochastic genetic evolution-based prediction model of received input voltage for underground imaging appli-

cations," in *2023 8th International Conference on Business and Industrial Research (ICBIR)*, 2023, pp. 549–555.

[20] B. P. Adedeji and G. Kabir, "A feedforward deep neural network for predicting the state-of-charge of lithium-ion battery in electric vehicles," *Decision Analytics Journal*, vol. 8, p. 100255, 2023.

[21] C. Y. Hsu, R. Xiong, N. Chen, J. Li, and N. Tsou, "Deep neural network battery life and voltage prediction by using data of one cycle only," *Applied Energy*, vol. 306, p. 118134, 2022.

[22] A. Rahman, V. Srikumar, and A. D. Smith, "Predicting electricity consumption for commercial and residential buildings using deep recurrent neural networks," *Applied Energy*, vol. 212, pp. 372–385, 2018.

[23] A. A. Ibrahim and N. H. El-Amary, "Particle swarm optimization trained recurrent neural network for voltage instability prediction," *Journal of Electrical Systems and Information Technology*, vol. 5, pp. 216–228, 2018.

[24] H. Hagmar, L. Tong, R. Eriksson, and L. A. Tuan, "Voltage instability prediction using a deep recurrent neural network," *IEEE Transactions on Power Systems*, vol. 36, no. 1, pp. 17–27, 2021.

[25] H. Fu and Y. Liu, "A deep learning-based approach for electrical equipment remaining useful life prediction," *Autonomous Intelligent Systems*, vol. 2, 2022.

[26] Y. Chen, "Voltages prediction algorithm based on lstm recurrent neural network," *Optik*, vol. 220, p. 164869, 2020.

[27] M. Jiao, D. Wang, and J. Qiu, "A gru-rnn based momentum optimized algorithm for soc estimation," *Journal of Power Sources*, vol. 459, p. 228051, 2020.

[28] F. Huo and C.-H. Chen, "The state of charge estimation based on gru for lithium-ion batteries," in *2022 IEEE 11th Global Conference on Consumer Electronics (GCCE)*, 2022, pp. 220–221.

[29] G. Cho, D. Zhu, and J. R. Campbell, "A comparative study of recurrent neural network architectures for battery voltage prediction," *SAE Technical Paper Series*, 2021.

[30] M. Abumohsen, A. Y. Owda, and M. Owda, "Electrical load forecasting using lstm, gru, and rnn algorithms," *Energies*, vol. 16, p. 2283, 2023.

[31] O. Kuras, "The capacitive resistivity technique for electrical imaging of the shallow subsurface," Ph.D. dissertation, University of Nottingham, 2002.

[32] R. Barika and O. Faust, "A review of automated sleep stage scoring," *Encyclopedia of Sleep and Circadian Rhythms*, pp. 63–73, 2023.

[33] R. S. DiPietro and G. D. Hager, "Deep learning: rnns and lstm," *Handbook of Medical Image Computing and Computer Assisted Intervention*, pp. 503–519, 2020.

[34] Z. Hamad and I. Abdulrahman, "Deep learning-based load forecasting considering data reshaping using matlab," *International Journal of Energy and Environmental Engineering*, vol. 13, pp. 853–869, 2022.

[35] S. Yang, X. Yu, and Y. Zhou, "Lstm and gru neural network performance comparison study: Taking yelp review dataset as an example,"

in *2020 International Workshop on Electronic Communication and Artificial Intelligence (IWECAI)*, 2020, pp. 98–101.

[36] X. Le, H. C. Ho, G. Lee, and S. Jung, "Application of long short-term memory (lstm) neural network for flood forecasting," *Water*, vol. 11, p. 1387, 2019.

[37] S. Kumar, L. Hussain, S. Banarjee, and M. Reza, "Energy load forecasting using deep learning approach-lstm and gru in spark cluster," in *2018 Fifth International Conference on Emerging Applications of Information Technology (EAIT)*, 2018, pp. 1–4.

[38] D. P. Kingma and J. Ba, "Adam: a method for stochastic optimization," 2014.

[39] T. Gupta and S. N. Sachdeva, "Recurrent neural network-based prediction of compressive and flexural strength of steel slag mixed concrete," *Neural Computing and Applications*, vol. 33, pp. 6951–6963, 2020.

Author 3 Dr. Ronnie S. Concepcion II is an outstanding young scientist and researcher associated with De La Salle University. In 2021, he completed his Ph.D. degree at De La Salle University and immediately joined the institution as an Associate Professor. His primary area of research revolves around the development of non-intrusive methods for crop phenotyping. His research focuses on using integrated machine vision and computational intelligence to investigate crops at the molecular, organelle, and system domains. By utilizing these innovative approaches, Dr. Concepcion aims to contribute to sustainable and precision agriculture practices. He is a member of the Institute of Electrical and Electronics Engineers (IEEE) and holds regular membership in the National Research Council of the Philippines (NRCP).

Author 1 Ms. Jonah Jahara Baun is a researcher associated with De La Salle University. In 2020, she received her B.Sc degree in Electronics and Communications Engineering from the Polytechnic University of the Philippines-Manila. Following her academic achievements, she joined De La Salle University in 2022 for her M.Sc degree of the same engineering field. Her main work revolves around the development of Capacitive Resistivity Underground Imaging System Equipment and Artificial Intelligence. Ms. Baun is a member of the Institute of Electrical and Electronics Engineers (IEEE) and an Associate Member at the National Research Council of the Philippines (NRCP).

Author 4 Ms. Kate Francisco is a researcher affiliated with De La Salle University (DLSU). She holds a B.Sc degree in Manufacturing Engineering from Bulacan State University and joined De La Salle University in 2021 to further his academic and professional pursuits. For now, her focus is in the development of Capacitive Resistivity Underground Imaging System Equipment. Ms. Francisco is a member of the Institute of Electrical and Electronics Engineers (IEEE) and an Associate Member at the National Research Council of the Philippines (NRCP).

Author 2 Mr. Adrian Genevie Janairo is a researcher affiliated with De La Salle University. In 2020, he received his B.Sc degree in Electronics and Communications Engineering from the University of Santo Tomas. Shortly after, he joined De La Salle University in 2021 for his graduate studies. His primary focus and main work revolve around the development of Capacitive Resistivity Underground Imaging System Equipment.

Author 5 Mr. Mike Louie Enriquez is a researcher associated with De La Salle University. He received his B.Sc degree in Manufacturing Engineering from Bulacan State University in 2018 and currently taking his Master's degree at DLSU for the same engineering field. His main focus lies in the development of Capacitive Resistivity Underground Imaging System Equipment. Mr. Enriquez is a member of the Institute of Electrical and Electronics Engineers (IEEE) and an Associate Member at the National Research Council of the Philippines (NRCP).

Author 6 Mr. R-Jay Relano received his B.Sc degree in Mechanical Engineering from Bulacan State University in 2010. In 2021, he joined De La Salle University for his M.Sc degree in Manufacturing Engineering, where he is currently affiliated. His main work involves being the engineer in charge of designing the mechanical component of a towed imaging system. This responsibility showcases his expertise in mechanical design and his ability to contribute to the development of advanced imaging systems.

Author 8 Dr. Argel Bandala is a distinguished academic and researcher associated with De La Salle University. He joined the university in 2012 and has made significant contributions to his field. In 2014, he received his Ph.D. degree from the same institution. His main focus lies in the development of a swarming algorithm for unmanned aerial vehicles (UAVs). Through his work, he explores innovative approaches to enable UAVs to operate collaboratively and autonomously in swarms. Dr. Bandala is a member of the Institute of Electrical and Electronics Engineers (IEEE).

Author 7 Dr. Edwin Sybingco distinguished academic and researcher affiliated with De La Salle University. He completed his Ph.D. degree at De La Salle University, highlighting his expertise and commitment to advancing knowledge in his field. His main area of work centers around the application of computer vision, machine learning, deep learning, robotics, and signal processing. Dr. Sybingco is a member of the Institute of Electrical and Electronics Engineers (IEEE).

Author 9 Dr. Ryan Rhay Vicerra is a distinguished academic and researcher affiliated with De La Salle University. In 2014, he completed his Ph.D. degree at De La Salle University, highlighting his expertise and commitment to advancing knowledge in his field. His main area of work centers around swarm intelligence for underwater swarm robot systems. He has dedicated his efforts to the development of an underwater swarm robot system, utilizing swarm intelligence techniques. Through his research, he aims to enhance the capabilities of underwater robotics and contribute to the exploration and understanding of aquatic environments. Dr. Vicerra is a member of the Institute of Electrical and Electronics Engineers (IEEE).